NMR Studies of Abasic Sites in DNA Duplexes: Deoxyadenosine Stacks into the Helix Opposite the Cyclic Analogue of 2-Deoxyribose†

Matthew W. Kalnik,‡ Chien-Neng Chang,§ Arthur P. Grollman,*,§ and Dinshaw J. Patel*,‡

Department of Biochemistry and Molecular Biophysics, College of Physicians and Surgeons, Columbia University, New York, New York 10032, and Department of Pharmacological Sciences, State University of New York at Stony Brook, Stony Brook, New York 11794

Received July 20, 1987; Revised Manuscript Received October 1, 1987

ABSTRACT: Proton and phosphorus NMR studies are reported for the complementary d(C-A-T-G-*A*-G-T-A-C)·d(G-T-A-C-*F*-C-A-T-G) nonanucleotide duplex (designated AP_F 9-mer duplex) which contains a stable abasic site analogue, F, in the center of the helix. This oligodeoxynucleotide contains a modified tetrahydrofuran moiety, isosteric with 2-deoxyribofuranose, which serves as a structural analogue of a natural apurinic/apyrimidinic site [Takeshita, M., Chang, C. N., Johnson, F., Will, S., & Grollman, A. P. (1987) *J. Biol. Chem. 262*, 10171-10179]. Exchangeable and nonexchangeable base and sugar protons, including those located at the abasic site, have been assigned in the complementary AP_F 9-mer duplex by recording and analyzing two-dimensional phase-sensitive NOESY data sets in H_2O and D_2O solution at low temperature (0 °C). These studies indicate that *A5* inserts into the helix opposite the abasic site F14 and stacks with flanking G4·C15 and G6·C13 Watson-Crick base pairs. Base-sugar proton NOE connectivities were measured through G4-*A5*-G6 on the unmodified strand and between the base protons of C15 and the sugar protons of the 5′-flanking residue F14 on the modified strand. These studies establish that all glycosidic torsion angles are *anti* and that the helix is right-handed at and adjacent to the abasic site in the AP_F 9-mer duplex. Two of the 16 phosphodiester groups exhibit phosphorus resonances outside the normal spectral dispersion indicative of altered torsion angles at two of the phosphate groups in the backbone of the AP_F 9-mer duplex.

The abasic site in DNA consists of a 2-deoxyribose residue linked to neighboring bases through 3′- and 5′-phosphodiester bonds:

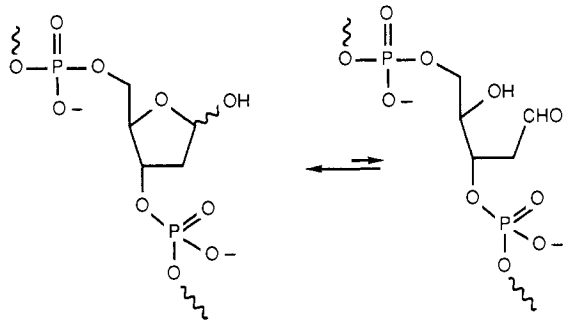

This biologically important lesion is created by selective hydrolysis of the N-glycosidic bond, a reaction that occurs spontaneously under physiological conditions (Lindahl & Nyberg, 1972) and is markedly accelerated by modification of purine residues at the N-3 and/or N-7 positions [reviewed by Loeb and Preston (1986)]. Abasic sites are also produced by the action of *N*-glycosylases, which remove abnormal bases from DNA (Lindahl, 1982; Weiss & Grossman, 1987).

DNA containing abasic sites lacks primary coding information. When these sites are copied or bypassed by DNA polymerases, misincorporation of bases occurs (Loeb & Kunkel, 1982). Thus, abasic sites may play an important role in spontaneous and chemically induced mutagenesis (Loeb, 1985; Loeb & Preston, 1986). Abasic sites in DNA are subject to a β-elimination reaction which leads to strand scission (Weiss & Grossman, 1987). The relative instability of these sites can be minimized by replacing the 2-deoxyribose moiety with 3-hydroxy-2-(hydroxymethyl)tetrahydrofuran (structure 1) (Millican et al., 1984; Takeshita et al., 1987). Oligodeoxynucleotides containing this cyclic analogue are substrates for several AP endonucleases (Takeshita et al., 1987) and DNA polymerases (Takeshita et al., 1987; Randall et al., 1987) and serve as models for the structural studies reported in this paper.

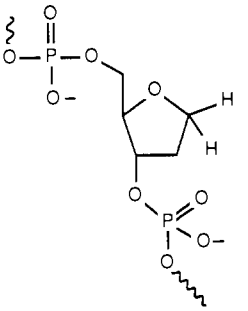

structure 1

The precise conformation of DNA at the abasic site has not been established. To obtain an initial solution to this problem, the structure and dynamics of an oligodeoxynucleotide duplex containing a single abasic site were probed at and adjacent to the site of modification. In this paper, we report two-dimensional NMR studies of the complementary nonanucleotide duplex d(C-A-T-G-*A*-G-T-A-C)·d(G-T-A-C-*F*-C-A-T-G) containing deoxyadenosine located opposite the abasic site in the center of the duplex (structure 2).

†This research was supported, in part, by a Columbia University Faculty start-up grant and NIH Grant CA-46533 to D.J.P. and NIH Grants CA 17395 and ESO4068 to A.P.G. NMR studies were conducted on instruments purchased with funds provided by Robert Woods Johnson Jr. Charitable Trust and the Matheson Foundation.

‡Columbia University.

§State University of New York at Stony Brook.

0006-2960/88/0427-0924$01.50/0

C1-A2-T3-G4-A5-G6-T7-A8-C9
G18-T17-A16-C15-F14-C13-A12-T11-G10

structure 2

Experimental Procedures

The numbering system of the complementary nonanucleotide strands in the d(C-A-T-G-*A*-G-T-A-C)·d(G-T-A-C-*F*-C-A-T-G) abasic 9-mer duplex is shown in structure 2.

Oligonucleotide Synthesis. The preparation and biological properties of modified deoxyoligonucleotides in which one of the nucleoside bases is replaced by a hydrogen atom at the C1 position of deoxyribose (structure 1) has been described (Takeshita et al., 1987). Oligodeoxynucleotides were assembled on a 5-μmol resin with a Vega (Du Pont) Coder 300 automated DNA synthesizer. When the position of the abasic site is reached during the synthesis, the appropriately protected tetrahydrofuran moiety was added in two portions. The remaining nucleotide units of the chain were then assembled. The yields were 98% at each coupling step.

4,4′-Dimethoxytrityl- (DMT-) modified oligodeoxynucleotides were adsorbed to a 30-cm C18 μBondapak analytical reverse-phase column and then eluted over 10 min with a 15–30% gradient of acetonitrile dissolved in 0.05 M triethylammonium acetate, pH 7.0. After deprotection and rechromatography, the principal UV-adsorbing product migrated as a single band when subjected to electrophoresis on 20% polyacrylamide gel in a buffer composed of 7 M urea, 100 mM tris(hydroxymethyl)aminomethane (Tris)–borate, and 10 mM ethylenediaminetetraacetic acid (EDTA) (pH 8.3) (Takeshita et al., 1987). The oligonucleotides were desalted by passage over a Sephadex G-25 column and the counterions exchanged for Na^+ by ion exchange.

Sample Preparation. A 1:1 stoichiometry of the complementary strands in the abasic 9-mer duplex was achieved by monitoring the cytidine H6 proton resonances during the gradual addition of the d(C-A-T-G-*A*-G-T-A-C) strand to the d(G-T-A-C-*F*-C-A-T-G) strand at 35 °C. At this temperature the duplex is melted into unstacked single strands, and the narrow resonances can be used to generate 1:1 stoichiometry of the two strands. The modified 9-mer duplex was dissolved in 0.4 mL of 0.1 M NaCl–10 mM phosphate aqueous solution at a concentration of $\sim$370 A_{260} units. The pH values recorded in D_2O were uncorrected pH meter readings.

NMR Experiments. Proton NMR spectra were recorded at 500 MHz with quadrature detection on a Bruker AM 500 spectrometer. Two-dimensional phase-sensitive (States et al., 1982) NOESY spectra (mixing time 120 ms) were recorded with a jump and return (90y, t, 90–y) pulse sequence (Plateau et al., 1982) for the preparation, mixing, and detection pulses. The carrier frequency was centered on the H_2O signal, and the waiting time, t, was optimized such that the imino and aromatic protons were excited equally. The time domain data sets consist of 1024 complex data points over a sweep width of 10000 Hz in the t_2 dimension. The repetition delay was 0.5 s. The free induction decays (FID's) were apodized with a 90°-shifted sine bell function zeroed to the 1024th point in the t_2 dimension and to the 256th point in the t_1 dimension. Both dimensions were also multiplied by an exponential function with 3-Hz line broadening before Fourier transformation. Each dimension was base line corrected with a fifth-order polynomial base line fitting routine supplied by Dr. Arthur Pardi (unpublished results) after Fourier transformation.

Correlated (COSY) data were recorded as two-dimensional magnitude data sets in D_2O by placing the carrier on the HOD resonance and using the decoupler channel to presaturate the residual HOD signal. Time domain data sets, consisting of 512 t_1 increments, were collected with a sweep width of 5000 Hz with 1024 complex data points in the t_2 dimension and a repetition delay of 1.5 s. Thirty-two scans were collected for each t_1 increment. The magnitude COSY data were apodized with an unshifted sine bell function zeroed to the 1024th point in the t_2 dimension and to the 512th point in the t_1 dimension prior to Fourier transformation.

Two-dimensional phase-sensitive NOESY spectra (mixing time 250 ms) were recorded in D_2O solution with the carrier frequency positioned on the residual HOD resonance. The decoupling channel was used to suppress the residual HOD resonance. The time domain data sets were accumulated over a sweep width of 5000 Hz with 1024 complex data points in the t_2 dimension and 256 complex data points in the t_1 dimension. The repetition delay was 1.5 s, and 32 scans were collected for each t_1 increment. The free induction decays were apodized with a 30°-shifted sine bell function at the 1024th point in the t_2 dimension and at the 256th point in the t_1 dimension and Fourier transformed in both dimensions.

One-dimensional difference NOE experiments were collected in H_2O with the 1–1 H_2O suppression pulse (Hore, 1983). The carrier frequency was shifted 6000 Hz downfield from the H_2O resonance and the 1–1 delay optimized for solvent suppression. We collected 2048 complex data points over a 20000-Hz sweep width with a 0.5-s repetition delay. Resonances of interest were irradiated for 200 ms with the decoupler channel. Data collection of the decoupled and control resonances was interleaved every 16 scans for a total of 3616 scans for each of the control and decoupled resonances. The FID's were subtracted after applying a line broadening of 3 Hz and Fourier transformed to obtain the NOE difference spectra.

One- and two-dimensional data sets were processed with FTNMR software (D. Hare, unpublished programs) on VAX 11-780 and micro VAX-II computers. Two-dimensional data sets were processed with the t_1 noise reduction routine of either Klevitt (1985) or Otting et al. (1986) and symmetrized prior to plotting on either ZETA 822 or HP 7475A plotters.

Results

The proton NMR spectra of the abasic 9-mer duplex (designated AP_F 9-mer duplex), recorded in 0.1 M NaCl–10 mM phosphate aqueous solution at $\sim$0 °C, demonstrate formation of a stable nonanucleotide duplex containing a central abasic site. The exchangeable proton spectrum (14–6 ppm) of the AP_F 9-mer duplex in H_2O, pH 6.0 at −5 °C, exhibits thymidine imino protons between 13.5 and 13.75 ppm, guanosine imino protons between 12.35 and 12.85 ppm, and nonexchangeable base and amino protons between 7 and 8.5 ppm (Figure 1A). The nonexchangeable proton spectrum (1–9 ppm) of the AP_F 9-mer duplex in D_2O, pH 7.3 at 5 °C, exhibits partially resolved narrow base and sugar proton resonances (Figure 1B). The observed resolution in the one-dimensional spectra suggests that the exchangeable and nonexchangeable protons could be assigned from an analysis of two-dimensional spectra.

Exchangeable Proton Spectra. The four thymidine imino protons are partially resolved while the four guanosine imino protons are fully resolved in the exchangeable proton spectrum of the AP_F 9-mer duplex, H_2O buffer, pH 6.0 at 0 °C (Figure 2). The exchange characteristics of the imino protons can be monitored by following their line widths as the temperature increases. We observe that all imino protons broaden significantly at 20 °C due to rapid exchange with solvent water

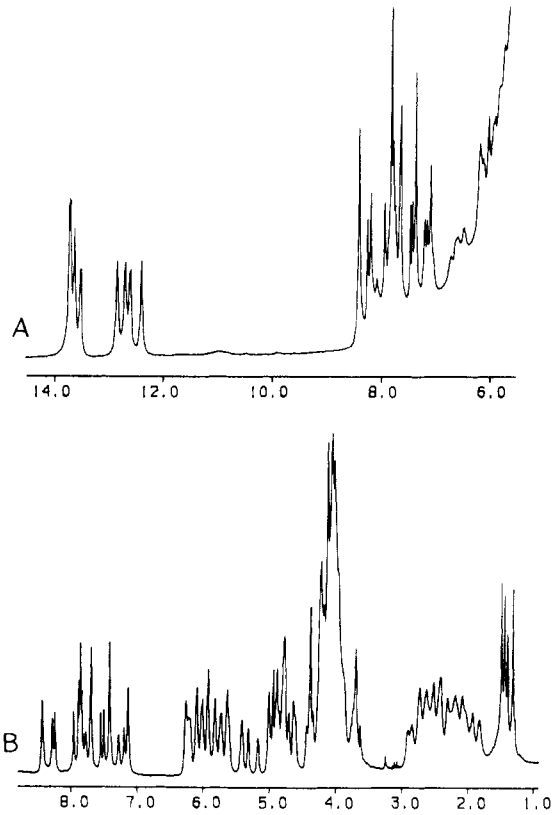

FIGURE 1: The 500-MHz proton NMR spectra of the AP_F 9-mer duplex in 0.1 M NaCl and 10 mM phosphate, aqueous solution. (A) The exchangeable proton spectrum (6–15 ppm) in H_2O, pH 6.0, at −5 °C. (B) The nonexchangeable proton spectrum (1.0–9.0 ppm) in D_2O, pH 7.3, at 5 °C.

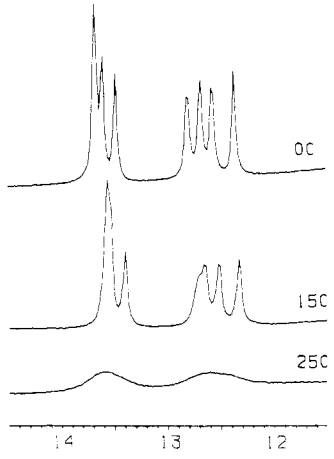

FIGURE 2: Temperature dependence of the exchangeable imino proton spectra (14.5–12.0 ppm) of the AP_F 9-mer duplex in 0.1 M NaCl and 10 mM phosphate, H_2O, pH 6.0, at 0, 15, and 25 °C.

at the onset of the melting transition.

The imino proton resonances have been assigned by recording a phase-sensitive NOESY (mixing time 120 ms) spectrum of the AP_F 9-mer duplex in 0.1 M NaCl, H_2O, pH 6.0 at −5 °C. Expanded contour plots of the phase-sensitive NOESY spectrum establishing distance connectivities in the symmetrical 12.0–14.5 ppm imino proton region are plotted in Figure 3A, and those establishing distance connectivities between the imino proton region (12.0–14.5 ppm) and the amino and base proton regions (6.5–9.0 ppm) are plotted in Figure 3B.

We can readily monitor the NOE cross-peaks between the thymidine imino and adenosine H2 protons within each of the four A·T base pairs (cross-peaks E, F, G, and H, Figure 3B)

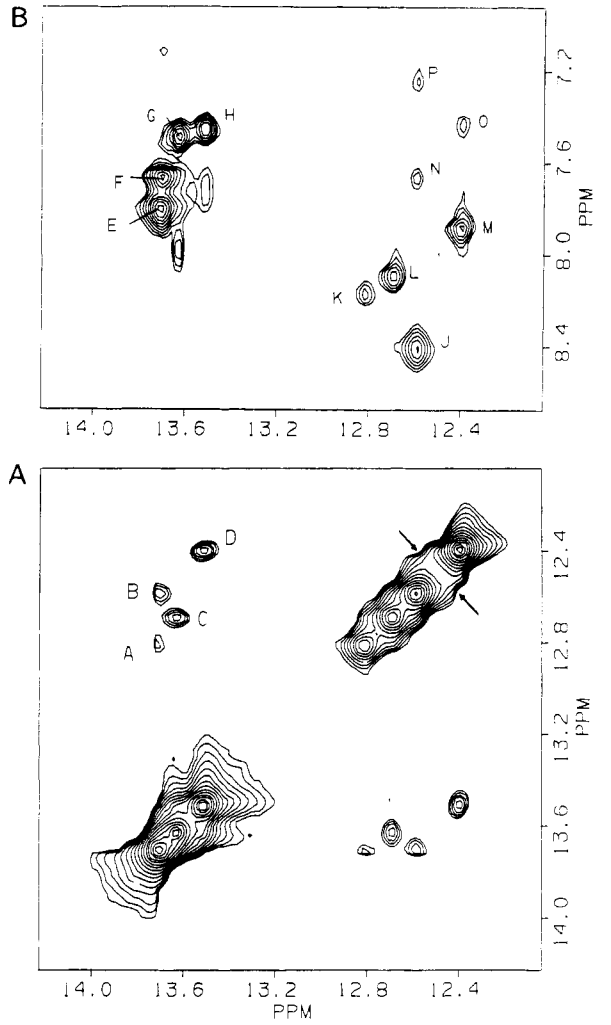

FIGURE 3: Expanded phase-sensitive NOESY (120-ms mixing time) contour plots of the AP_F 9-mer duplex in 0.1 M NaCl and 10 mM phosphate, H_2O, pH 6.0, at −5 °C. (A) Cross-peaks establishing connectivities between imino protons in the symmetrical 12.4–14.0 ppm spectral range. (B) Cross-peaks establishing connectivities between the imino protons (12.4–14.0 ppm) and the base and amino protons (7.4–8.8 ppm). The cross-peaks A–P are discussed in the text.

and the NOE cross-peaks between the guanosine imino and hydrogen-bonded cytidine amino protons within each of the four G·C base pairs (cross-peaks J, K, L, and M, Figure 3B) in the AP_F 9-mer duplex. This result establishes that all A·T and G·C base pairs are stabilized by Watson–Crick pairing in the AP_F 9-mer duplex at low temperature.

Thymidine and guanosine imino protons in the AP_F 9-mer duplex can be assigned by the procedure outlined below. The H2 protons of the five adenosines are well resolved in the base proton spectral region of the AP_F 9-mer duplex in D_2O at 5 °C and can be selectively observed in an inversion recovery experiment (Figure 4). The adenosine H2 protons can be assigned to positions A2, A5, A8, A12, and A16 in the AP_F 9-mer duplex by monitoring NOEs to nearby assigned sugar H1′ protons (see next section). These assignments are listed under each resonance in the spectra in Figure 4.

The observed NOE cross-peaks from individual assigned adenosine H2 protons to their corresponding thymidine imino protons within each of the A·T base pairs (cross-peaks E, F, G, and H, Figure 3B) permit assignment of the imino protons of T3, T7, T11, and T17 in the AP_F 9-mer duplex. Further, NOE cross-peaks between imino protons on adjacent A·T and G·C base pairs (cross-peaks A, B, C, and D, Figure 3A) permit

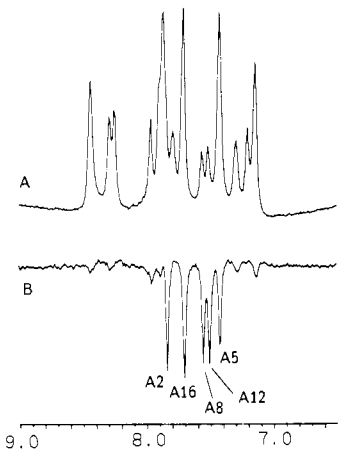

FIGURE 4: (A) Base proton region of the nonexchangeable proton spectrum of the AP_F 9-mer duplex in 0.1 M NaCl and 10 mM phosphate, D_2O, pH 7.3, at 5 °C. (B) An inversion recovery experiment of the same spectral region (0.9-s delay between 180° and 90° pulses). The adenosine H2 protons which exhibit the longest T_1 relaxation times are inverted under conditions where the remaining base protons are nulled. The assignments of the H2 protons to specific adenosines are listed under each resonance.

Table I: Exchangeable Proton Chemical Shifts in the AP_F 9-mer Duplex at −5 °C[a]

	chemical shifts (ppm)				
base pair	T-H3	G-H1	C-H4[b]	C-H4[c]	A-H2
C1·G18		12.82	8.17	7.08	
A2·T17	13.71				7.80
T3·A16	13.69				7.66
G4·C15		12.58	8.41	7.23	
A5·F14					7.43
G6·C13		12.38	7.88	6.64	
T7·A12	13.51				7.45
A8·T11	13.62				7.49
C9·G10		12.68	8.10	6.79	

[a] In 0.1 M NaCl and 10 mM phosphate, H_2O, pH 6.0. [b] Hydrogen-bonded cytidine amino protons. [c] Exposed cytidine amino protons.

assignment of the imino protons of G4, G6, G10, and G18 in the AP_F 9-mer duplex. Finally, NOE cross-peaks from individual assigned guanosine imino protons to their corresponding hydrogen-bonded cytidine amino protons within each of the G·C base pairs (cross peaks J, K, L, and M, Figure 3B) permit assignment of the hydrogen-bonded amino protons of C1, C9, C13, and C15 in the AP_F 9-mer duplex. Specific assignments are listed in Table I.

Imino, hydrogen-bonded cytidine amino, and adenosine H2 proton assignments in the AP_F 9-mer duplex at −5 °C listed in Table I are confirmed by the observed cross-peaks between guanosine imino protons and adenosine H2 protons on adjacent base pairs (cross peaks N and O, Figure 3B).

We have also undertaken one-dimensional NOE experiments to establish whether A5 opposite the abasic site F14 stacks into the helix or loops out into solution in the AP_F 9-mer duplex at −5 °C. Specifically, we searched for NOEs between the H2 proton of A5 and the imino protons of flanking G4·C15 and G6·C13 base pairs. Experimentally, 0.2-s saturation of the 12.58 ppm imino proton of G4 results in NOEs at the 8.42 ppm hydrogen-bonded cytidine amino protons of C15 within the G4·C15 base pair, at the 13.69 ppm thymidine imino and 7.66 ppm adenosine H2 of the flanking T3·A16 base pair in one direction, and at the 7.40 ppm adenosine H2 of A5 in the other direction (Figure 5B). Similarly, saturation of the 12.38 ppm imino proton of G6 results in NOEs at the 7.88 ppm hydrogen-bonded cytidine amino protons of C13 within the G6·C13 base pair, at the 13.50 ppm thymidine imino and 7.44

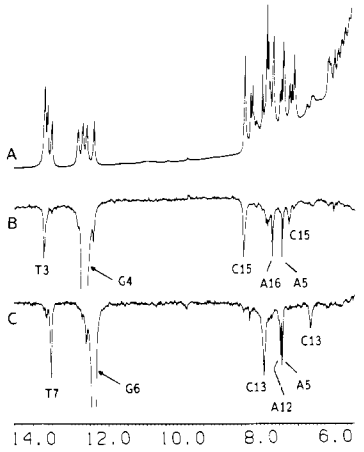

FIGURE 5: (A) The 500-MHz proton NMR spectrum (6–14 ppm) of the AP_F 9-mer duplex in 0.1 M NaCl and 10 mM phosphate, H_2O, pH 6.0, at −5 °C. Difference spectra following 0.2-s saturation of (B) the 12.58 ppm imino proton of the G4·C15 base pair and (C) the 12.38 ppm imino proton of the G6·C13 base pair. The saturated resonance is designated by an arrow.

ppm adenosine H2 of flanking T7·A12 base pair in one direction, and at the 7.40 ppm adenosine H2 of A5 in the other direction (Figure 5C). These studies establish that the guanosine imino proton of G4 as well as that of G6 exhibits NOEs to the H2 protons of A5 in the AP_F 9-mer duplex at low temperature. It should also be noted that an NOE was not detected between the imino protons of G4·C15 and G6·C13 (see arrow in Figure 3A), consistent with a stacked A5 residue acting as a spacer between these base pairs.

Nonexchangeable Proton Spectra. The nonexchangeable base and sugar protons in the AP_F 9-mer duplex in 0.1 M NaCl, D_2O, pH 7.3, have been assigned by recording two-dimensional through-bond COSY and through-space NOESY data sets at 5 °C.

The expanded NOESY contour plot, establishing distance connectivities between the base protons (7.1–8.5 ppm) and the sugar H1′ and sugar H3′ protons (4.4–6.4 ppm) in the AP_F 9-mer duplex, is plotted in duplicate in Figures 6 and 7. Previous studies demonstrate that the purine H8 and pyrimidine H6 protons exhibit NOEs to their own and 5′-flanking sugar H1′ protons in right-handed DNA and that the same connectivities also hold true for the H3′ protons and H2′,2″ protons (Hare et al., 1983; Scheek et al., 1984; Weiss et al., 1984). The 5′-terminal base can be readily identified since NOEs from the base are detected only at its own sugar protons. Further, the H5′,5″ sugar protons of the 5′-terminal nucleotide are well resolved from the remaining superpositioned H5′,5″ sugar protons of the oligonucleotide duplex. We can readily trace the chain without interruption in both the H1′ (5.6–6.4 ppm) and the H3′ (4.5–5.1 ppm) spectral regions for the unmodified strand C1-A2-T3-G4-*A5*-G6-T7-A8-C9 (Figure 6). The tracing through the G4-*A5*-G6 segment can be followed and is consistent with A5 stacking into the duplex. We do note, however, that the NOE between the H8 proton of G6 and the H1′ proton of A5 is weak, indicative of a structural perturbation at the abasic site. We can also trace the chain through the sugar H1′ region as well as the sugar H3′ region from G10 to C13 and from C15 to G18 in the abasic site containing strand G10-T11-A12-C13-*F14*-C15-A16-T17-G18 with the interruption reflecting the missing base on F14 (Figure 7). A one-dimensional slice through the H6 of C15 exhibits NOEs to the H1′, H2′, H2″, and H3′ sugar protons of C15 and to the H2′, H2″, and H3′ protons of 5′-flanking F14 in the AP_F 9-mer duplex (Figure 8). These results

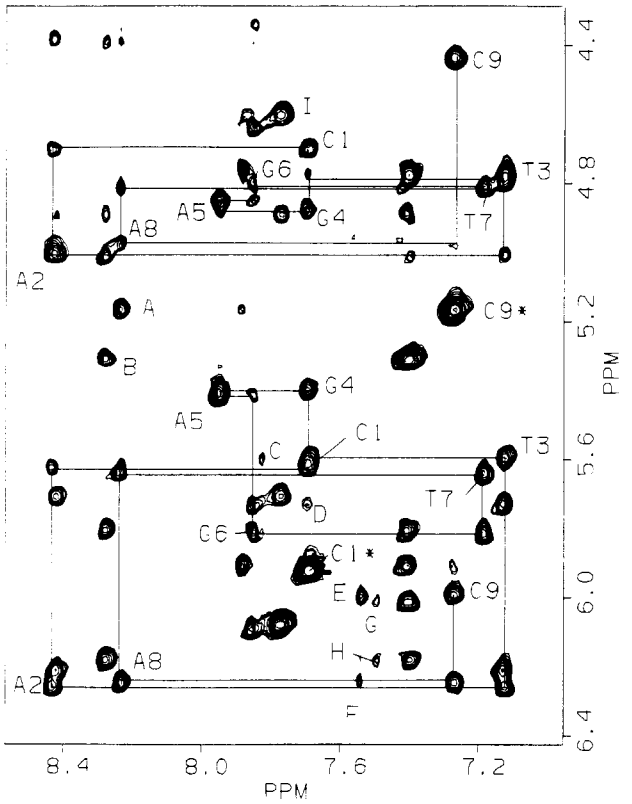

FIGURE 6: Expanded contour plots of the phase-sensitive NOESY spectrum (mixing time 250 ms) of the AP_F 9-mer duplex in 0.1 M NaCl and 10 mM phosphate, D_2O, pH 7.3, at 25 °C. Distance connectivities between the base protons (7.0–8.5 ppm) and the sugar H1′ and cytidine H5 protons (5.1–6.4 ppm) and the sugar H3′ protons (4.4–5.1 ppm). The cytidine H6–H5 cross-peaks are designated by asterisks. The cross-peaks A–I are discussed in the text. The lines follow connectivities between adjacent base protons through their intervening sugar H1′ or sugar H3′ protons in the d(C1-A2-T3-G4-A5-G6-T7-A8-C9) strand of the AP_F 9-mer duplex.

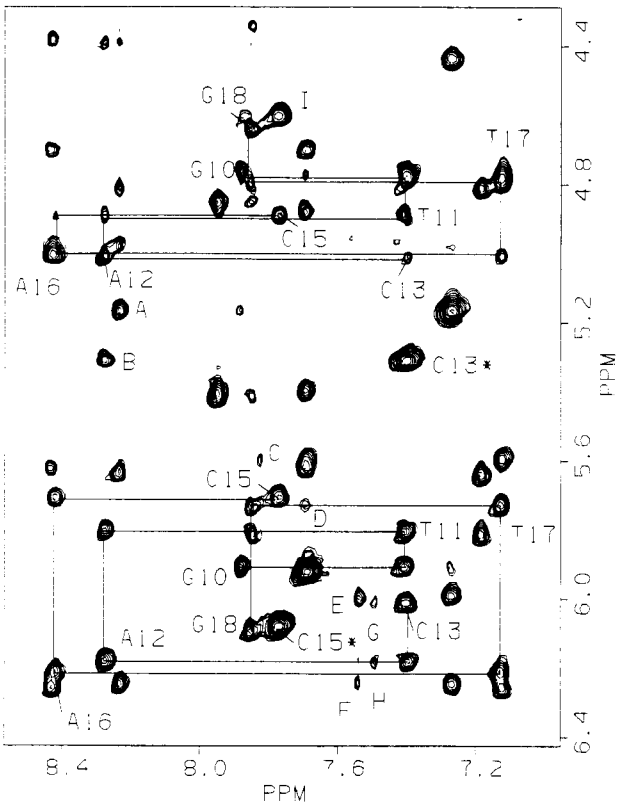

FIGURE 7: Same expanded NOESY contour plot as in Figure 6. The lines follow connectivities between adjacent base protons through their intervening sugar H1′ or sugar H3′ protons in the d(G10-T11-A12-C13-F14-C15-A16-T17-G18) strand of the AP_F 9-mer duplex.

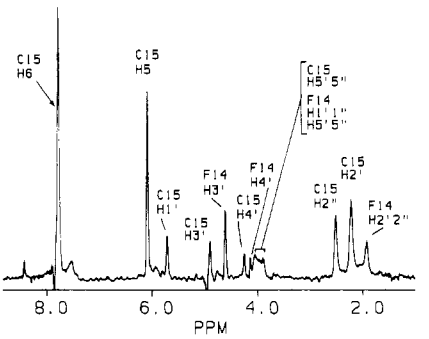

FIGURE 8: One-dimensional slice through the H6 proton on C15 in the phase-sensitive NOESY (250-ms mixing time) spectrum of the AP_F 9-mer duplex in 0.1 M NaCl and 10 mM phosphate, D_2O, pH 7.3, at 25 °C. The C15 H6 resonance is indicated by an arrow, and the observed NOEs are assigned to specific base and sugar protons on C15 and sugar protons on F14.

establish that both strands in the AP_F 9-mer duplex are right-handed both at the abasic site and its flanking base pair regions.

We also detect NOE cross-peaks between purine H8 and pyrimidine H5/CH_3 protons on adjacent bases for purine-(3′–5′)pyrimidine steps in the AP_F 9-mer duplex. These include NOE connectivities for the A2-T3, G6-T7, A8-C9 (cross-peak A, Figure 6), G10-T11, A12-C13 (cross-peak B, Figure 6), and A16-T17 steps and independently demonstrate that the AP_F 9-mer duplex is a right-handed helix in solution.

Further support for formation of a right-handed helix comes from the observed NOEs between the adenosine H2 proton and the sugar H1′ protons on the same and partner strands. We can detect such resolved cross-peaks for the H2 protons of A2 (cross-peak C, Figure 6), A8 (cross-peaks E and F, Figure 6), A12 (cross-peaks G and H, Figure 6), and A16 (cross-peak D, Figure 6).

The sugar proton chemical shifts at the abasic site F14 in the AP_F 9-mer duplex can be assigned through analysis of expanded regions of the two-dimensional contour plots relating the 3.5–4.5 ppm region with the 1.5–4.3 ppm region of the magnitude COSY spectrum (Figure 9A) and the phase-sensitive NOESY spectrum (Figure 9B). The abasic site sugar H1′,H1″ protons resonate at 3.87 and 3.96 ppm (we cannot distinguish between H1′ and H1″ at this time) and exhibit through-bond (cross-peaks A and B, Figure 9A) and through-space (cross-peaks A and B, Figure 9B) connectivities to the superpositioned abasic H2′,H2″ protons at 1.92 ppm. The abasic H2′,H2″ protons exhibit, in turn, through-bond (cross-peak C, Figure 9A) and through-space (cross-peak C, Figure 9B) connectivities to the abasic H3′ protons at 4.61 ppm. In addition, COSY (cross-peak D, Figure 9A) and NOESY (cross-peak D, Figure 9B) cross-peaks between the 4.14 ppm abasic H4′ proton and the abasic H3′ proton provides a complete assignment of the sugar proton chemical shifts of the abasic site F14 in the AP_F 9-mer duplex (Table II).

Phosphorus Spectrum. We have recorded the 121.5-MHz proton-decoupled phosphorus spectrum of the AP_F 9-mer duplex in 0.1 M phosphate, D_2O, pH 7.3, at 5 °C. There are 16 backbone phosphates in the AP_F 9-mer duplex, and the majority of their resonances are dispersed between 4.0 and 4.5 ppm in the range characteristic of unperturbed phosphodiester backbone (Figure 10). In addition, we observe a narrow phosphorus resonance at 3.75 ppm and a broad resonance at 3.25 ppm, which is indicative of altered conformations at two

Table II: Nonexchangeable Proton Chemical Shifts in the AP_F 9-mer Duplex at 5 °C[a]

	chemical shifts (ppm)								
	H8	H2	H6	H5/CH_3	H1′	H2′	H2″	H3′	H4′
C1			7.69	5.92	5.62	2.02	2.42	4.70	4.04
A2	8.43	7.84			6.25	2.74	2.90	5.00	4.40
T3			7.12	1.45	5.59	1.82	2.14	4.78	4.08
G4	7.69				5.40	2.42	2.42	4.88	4.24
A5	7.95	7.42			5.41	2.44	2.53	4.85	4.26
G6	7.85				5.81	2.57	2.72	4.80	4.19
T7			7.18	1.40	5.64	2.08	2.41	4.82	4.24
A8	8.23	7.55			6.24	2.62	2.84	5.00	4.40
C9			7.27	5.17	5.99	2.09	2.09	4.44	3.97
G10	7.88				5.91	2.62	2.73	4.76	4.19
T11			7.41	1.32	5.80	2.18	2.51	4.88	4.24
A12	8.27	7.51			6.18	2.66	2.83	5.01	4.40
C13			7.40	5.31	6.01	2.18	2.31	4.78	4.21
F14					3.87, 3.96	1.92	1.92	4.61	4.14
C15			7.77	6.08	5.71	2.22	2.51	4.89	4.24
A16	8.42	7.70			6.21	2.73	2.91	5.01	4.40
T17			7.12	1.49	5.73	1.82	2.26	4.79	4.09
G18	7.85				6.09	2.30	2.57	4.64	4.14

[a] In 0.1 M NaCl and 10 mM phosphate, D_2O, pH 7.3.

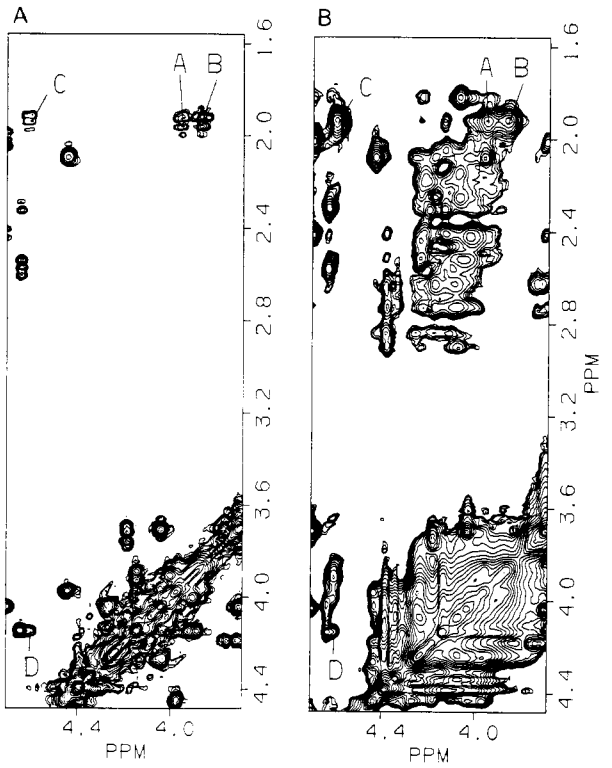

FIGURE 9: Two-dimensional NMR contour plots of the expanded spectral region establishing connectivities between protons in the 3.4–4.5 ppm region and the 1.6–4.4 ppm spectral region in the AP_F 9-mer duplex in 0.1 M NaCl and 10 mM phosphate, D_2O, pH 7.3, at 5 °C. (A) Magnitude COSY spectrum; (B) phase-sensitive (250-ms mixing time) NOESY spectrum.

of the backbone phosphates in the AP_F 9-mer duplex (Figure 10).

Discussion

Introduction of an abasic site in the center of the complementary nonanucleotide duplex is associated with helix destabilization. For this reason, our NMR studies on the 9-mer duplex containing the abasic site (structure 2) in aqueous solution were performed at temperatures between −5 and 5 °C.

The present NMR studies were undertaken with the eventual goal of defining structural features of the abasic site and adjacent base pairs in solution. In such an approach the first

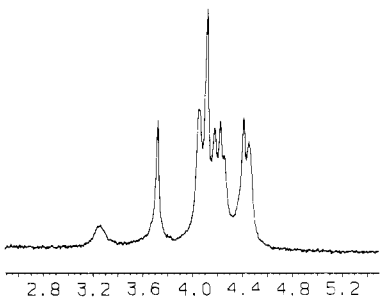

FIGURE 10: Proton Waltz-decoupled 121-MHz ^{31}P spectrum of the AP_F 9-mer duplex in 0.1 M NaCl and 10 mM phosphate, D_2O, pH 7.3, at 5 °C.

step is to assign the majority of the base and sugar protons on the unmodified and modified strands of the complementary AP_F 9-mer duplex. This was achieved through analysis of through-space NOESY data sets in H_2O and D_2O solution supplemented and, where necessary, by through-bond COSY spectra. These proton chemical shifts are listed in Tables I and II and include the proton chemical shifts of the sugar protons of the F14 abasic site.

Base Pairing. The imino protons of oligonucleotide duplexes represent sensitive markers for base pairing. NOE connectivities involving imino protons across the base pair permit differentiation of Watson–Crick from Hoogsteen base pairs. We detect four partially resolved thymidine imino and four well-resolved guanosine imino protons in the AP_F 9-mer duplex in 0.1 M NaCl, H_2O, pH 6.0, at −5 °C (Figure 1A), demonstrating formation of eight base pairs at low temperature. The observed NOEs between the thymidine imino and adenosine H2 protons establish Watson–Crick A·T pairing while the observed NOEs between the guanosine imino and hydrogen-bonded cytidine amino protons establish Watson–Crick G·C pairing in the AP_F 9-mer duplex at low temperature (Figure 3B). These studies establish the presence of intact Watson–Crick G4·C15 and G6·C13 base pairs on either side of the abasic site in the AP_F 9-mer duplex at low temperature.

We did not observe a NOE between the imino protons of G4·C15 and G6·C13 in the phase-sensitive NOESY spectrum of the AP_F 9-mer duplex at −5 °C (Figure 3A). This observation suggests that A5·F14 acts at a "spacer" between the G4·C15 and G6·C13 base pairs in the AP_F 9-mer duplex at low temperature.

Base Stacking and Helix Handedness. The observed NOE

connectivities between the base (purine H8 or pyrimidine H6) protons and their own and 5′-linked sugar (H1′, H2′,2″, and H3′) protons in the AP_F 9-mer duplex in 0.1 M NaCl, D_2O, 5 °C (Figures 6 and 7), establish the presence of a stacked right-handed helix in aqueous solution. This conclusion is reinforced by the directionality of the NOEs between (a) adjacent base protons in purine(3′–5′)pyrimidine steps and (b) adenosine H2 protons and sugar H1′ protons on the same and partner strands (Figures 6 and 7).

A5 Stacks into the Helix. The orientation of A5 in the AP_F 9-mer duplex is established by experiments designed to differentiate between a stacked and a looped-out A5 opposite the abasic site. The imino proton of G4 exhibits NOEs of similar magnitude to the adenosine H2 protons of adjacent A5 and A16 (Figure 5B). The imino proton of G6 exhibits NOEs of similar magnitude to adenosine H2 protons of adjacent A5 and A12 (Figure 5C) in the AP_F 9-mer duplex (structure 2) at −5 °C. These studies establish that A5 inserts into the helix, stacks with adjacent G4·C15 and G6·C13 base pairs, and places constraints on the orientation of A5 relative to the flanking G·C base pairs in the AP_F 9-mer duplex. The observed base to sugar NOEs also establish an *anti*-glycosidic torsion angle orientation for the A5 residue stacked into the helix.

We can readily trace connectivities between purine H8 protons and their own and 5′-flanking sugar protons in the G4-*A5*-G6 segment of the AP_F 9-mer duplex at 5 °C (Figure 8), consistent with stacking of A5 between G4 and G6 bases in the unmodified strand. The weak NOE between the H8 of G6 and the H1′ of A5 suggests a perturbation in the helix at the A5-G6 step.

The 7.95 ppm chemical shift of the H8 of A5 is upfield from the 8.2–8.45 ppm chemical shifts of the H8 protons of the four other adenosines in the AP_F 9-mer duplex (Table II), and the 7.42 ppm chemical shift of the H2 of A5 is the most upfield of the adenosine H2 protons in the AP_F 9-mer duplex (Table II). Upfield shifts are associated with stacking interactions, and A5 is flanked by the purines G4 and G6 in the AP_F 9-mer duplex.

Abasic Site F14. We have identified and assigned the abasic site F14 sugar protons in the AP_F 9-mer duplex at 5 °C. The absence of a base shifts the sugar H1′,H1″ protons of F14 upfield to 3.87 and 3.96 ppm relative to the 5.4–6.2 ppm chemical shift range for unperturbed sugar H1′ protons in oligonucleotide duplexes (Figure 9). The sugar (H1′, H2′,2″, H3′, and H4′) proton chemical shifts in the unmodified tetrahydrofuran moiety of F14 in the AP_F 9-mer duplex are listed in Table II.

Right handedness of the AP_F 9-mer duplex is also maintained at the abasic site since we detect NOEs from the H6 proton of C15 to its own and 5′-flanking F14 sugar protons in the AP_F 9-mer duplex at low temperature (Figure 8).

The two downfield-shifted resonances in the phosphorus spectrum of the AP_F 9-mer duplex at 5 °C (Figure 10) have established structural perturbations at two backbone phosphates in the vicinity of the abasic site. Further interpretation of this effect must await assignment of the shifted resonances to specific phosphates in the backbone of the AP_F 9-mer duplex.

Biological Implications. Experimental evidence implicating abasic sites as intermediates in spontaneous and induced mutagenesis has been reviewed by Loeb and Preston (1986). The precise conformation of DNA at the site of these lesions may determine the specific type of mutation produced. For example, retention of a right-handed helical structure, as demonstrated in the present study, could lead to erroneous base substitution since dAMP is preferentially incorporated opposite abasic sites in vitro and in vivo (Sagher & Strauss, 1983). Alternatively, if the base located opposite the abasic site rotates to an extrahelical position with stacking of base pairs located on either side of the lesion (Fresco & Alberts, 1960), a base deletion (frameshift) mutation might occur.

Efficient repair of abasic sites in DNA is essential to the integrity of living organisms. AP endonucleases locate and remove these potentially lethal lesions from the genetic material (Lindahl, 1982; Weiss & Grossman, 1987). The 2-deoxyribose residue is unlikely to play a significant role in the recognition process if the right-handed helix persists under physiological conditions. Alternatively, recognition of abasic sites by AP endonucleases could depend on the distortion of helical structure created by loss of the base and be experienced by the enzyme through alterations in the phosphodiester backbone at or near the abasic position. Structural investigations of the backbone structure in this region are currently under way.

Our studies indicate that duplex DNAs are capable of retaining right-handed helical structure even after removal of a base, raising the question as to the physical occupancy of the vacated space. This cavity could also provide a recognition site for the AP endonucleases. Duplex structures are destabilized by the introduction of an abasic site (Millican et al., 1984), and there appears to be considerable flexibility of such structures under physiological conditions (Pochet et al., 1986). The conformation of DNA is influenced by the ionic environment and the presence of proteins which bind to DNA (Zacharias et al., 1982). Interactions with DNA polymerase (Muise & Holler, 1985) may also contribute significantly to the final conformation of DNA containing abasic sites.

ACKNOWLEDGMENTS

We gratefully acknowledge the assistance of Robert Rieger in the large-scale preparation of modified oligodeoxynucleotides.

REFERENCES

Boelens, R., Scheek, R. M., Dijkstra, K., & Kaptein, R. (1985) *J. Magn. Reson. 62*, 378–386.

Fresco, J. R., & Alberts, B. M. (1960) *Proc. Natl. Acad. Sci. U.S.A. 46*, 311–321.

Hare, D. R., Wemmer, D. E., Chou, S. H., Drobny, G., & Reid, B. R. (1983) *J. Mol. Biol. 171*, 319–336.

Hore, P. J. (1983) *J. Magn. Reson. 55*, 283–300.

Klevitt, R. E. (1985) *J. Magn. Reson. 62*, 551–555.

Lindahl, T. (1982) *Annu. Rev. Biochem. 51*, 61–87.

Lindahl, T., & Nyberg, B. (1972) *Biochemistry 11*, 3610–3618.

Loeb, L. A. (1985) *Cell (Cambridge, Mass.) 40*, 483–484.

Loeb, L. A., & Kunkel, T. A. (1982) *Annu. Rev. Biochem. 52*, 429–547.

Loeb, L. A., & Preston, B. D. (1986) *Annu. Rev. Genet. 20*, 201–230.

Millican, T. A., Mock, G. A., Chauncey, M. A., Patel, T. P., Eaton, M. A. W., Gunning, J., Cutbush, S. D., Neidele, S., & Mann, J. (1984) *Nucleic Acids Res. 12*, 7435–7453.

Muise, O., & Holler, E. (1985) *Biochemistry 24*, 3618–3622.

Otting, G., Widmer, H., Wagner, G., & Wuthrich, K. (1986) *J. Magn. Reson. 66*, 187–193.

Plateau, P., & Gueron, M. (1982) *J. Am. Chem. Soc. 104*, 7310–7311.

Pochet, S., Huynh-Dinh, T., Neumann, J.-M., Tran-Dinh, S., Adam, S., Taboury, J., Taillandier, E., & Igolen, J. (1986)

Nucleic Acids Res. 14, 1107–1126.
Randall, S. K., Eritja, R., Kaplan, B., Petruska, J., & Goodman, M. F. (1987) *J. Biol. Chem. 262*, 6864–6870.
Sagher, D., & Strauss, B. (1983) *Biochemistry 22*, 4518–4526.
Scheek, R. M., Boelens, R., Russo, N., van Boom, J. H., & Kaptein, R. (1984) *Biochemistry 23*, 1371–1376.
States, D. J., Haberkorn, R. A., & Ruben, D. J. (1982) *J. Magn. Reson. 48*, 286–292.
Takeshita, M., Chang, C. N., Johnson, F., Will, S., & Grollman, A. P. (1987) *J. Biol. Chem. 262*, 10171–10179.
Weiss, B., & Grossman, L. (1987) *Adv. Enzymol. Relat. Areas Mol. Biol. 60*, 1–34.
Weiss, M. A., Patel, D. J., Sauer, R. T., & Karplus, M. (1984) *Proc. Natl. Acad. Sci. U.S.A. 81*, 130–134.
Zacharias, W., Larson, J. E., Klysik, J., Stirdivant, S. M., & Wells, R. D. (1982) *J. Biol. Chem. 257*, 2775–2782.

Crystal and Solution Structures of the B-DNA Dodecamer d(CGCAAATTTGCG) Probed by Raman Spectroscopy: Heterogeneity in the Crystal Structure Does Not Persist in the Solution Structure†

J. M. Benevides,‡ A. H.-J. Wang,§ G. A. van der Marel,‖ J. H. van Boom,‖ and G. J. Thomas, Jr.*,‡

Division of Cell Biology and Biophysics, School of Basic Life Sciences, University of Missouri—Kansas City, Kansas City, Missouri 64110, Department of Biology, Massachusetts Institute of Technology, Cambridge, Massachusetts 02139, and Gorlaeus Laboratory, Leiden State University, 2300RA Leiden, The Netherlands

Received June 8, 1987; Revised Manuscript Received September 22, 1987

ABSTRACT: The self-complementary dodecamer d(CGCAAATTTGCG) crystallizes as a double helix of the B form and manifests a Raman spectrum with features not observed in Raman spectra of either DNA solutions or wet DNA fibers. A number of Raman bands are assigned to specific nucleoside *sugar* and *phosphodiester* conformations associated with this model B-DNA crystal structure. The Raman bands proposed as markers of the crystalline B-DNA structure are compared and contrasted with previously proposed markers of Z-DNA and A-DNA crystals. The results indicate that the three canonical forms of DNA can be readily distinguished by Raman spectroscopy. *However, unlike Z-DNA and A-DNA, which retain their characteristic Raman fingerprints in aqueous solution, the B-DNA Raman spectrum is not completely conserved between crystal and solution states.* The Raman spectra reveal greater heterogeneity of nucleoside conformations (sugar puckers) in the DNA molecules of the crystal structure than in those of the solution structure. The results are consistent with conversion of one-third of the dG residues from the C2′-endo/anti conformation in the solution structure to another conformation, deduced to be C1′-exo/anti, in the crystal. The dodecamer crystal also exhibits unusually broad Raman bands at 790 and 820 cm^{-1}, associated with the geometry of the phosphodiester backbone and indicating a wider range of (α, ζ) backbone torsion angles in the crystal than in the solution structure. The results suggest that backbone torsion angles in the CGC and GCG sequences, which flank the central AAATTT sequence, are significantly different for crystal and solution structures, the former containing the greater diversity. The Raman data also suggest no significant change in the geometry of the central AAATTT domain between crystal and solution structures.

Methods of single-crystal X-ray diffraction analysis have provided high-resolution structures of a number of DNA oligomers in left-handed Z and right-handed A conformations (Wang et al., 1979, 1982; Wang & Rich, 1985; Shakked et al., 1983; McCall et al., 1985). Typically, the nucleotide repeat of A-DNA and the dinucleotide repeat of Z-DNA exhibit characteristic backbone conformations and, with the possible exception of terminal residues, a regularly repeating pattern of nucleoside sugar puckers. Many conformational properties of the Z and A families of DNA structure are also not particularly sensitive to the base sequence. On the other hand, the X-ray-determined secondary structure of the dodecamer sequence d(CGCGAATTCGCG), which has been recognized as that of B-DNA, manifests much less regularity in helix parameters and nucleoside conformations (Wing et al., 1980). Refinement of this structure by Dickerson and Drew (1981) has revealed a broader distribution of sugar puckers and base orientations than ordinarily found in oligomeric Z- and A-DNA crystals. It is not known whether such "microheterogeneity" of structure is a fundamental property of the B form of DNA, an attribute of the particular dodecamer sequence investigated, or a consequence of solvent–helix and helix–helix interactions in the crystal. In order to address questions of this sort, we are examining the crystal and solution structures of several sequences selected as candidates to form right-handed double helices of the B form. This paper reports the use of laser Raman spectroscopy to investigate the conformation of one such sequence, d(CGCAAATTTGCG), in both its crystal and its aqueous solution states.

The target sequence, d(CGCAAATTTGCG), is similar to that investigated by Dickerson and co-workers (Wing et al., 1980). Its composition differs only in 2 of the 12 nucleotide positions, with A replacing G at the fourth residue and T replacing C at the ninth residue from the 5′ end. The double

† Part XXXII in the series "Raman Spectral Studies of Nucleic Acids". This work was supported by grants from the National Institutes of Health (G.J.T. and A.H.-J.W.) and by a grant from the Burroughs Wellcome Co. (A.H.-J.W.).
* Author to whom correspondence should be addressed.
‡ University of Missouri—Kansas City.
§ Massachusetts Institute of Technology.
‖ Leiden State University.

0006-2960/88/0427-0931$01.50/0